Tetrahedral colloidal clusters from random parking of bidisperse spheres

Supplementary Information for "Tetrahedral colloidal clusters from random parking of bidisperse spheres"

Nicholas B. Schade, Miranda C. Holmes-Cerfon, Elizabeth R. Chen, Dina Aronzon, Jesse W. Collins, Jonathan A. Fan, Federico Capasso, Vinothan N. Manoharan

1 Electrostatic interaction experiments

Charged colloidal polystyrene spheres were purchased from Invitrogen as "IDC surfactant-free latex" in batches as listed in Table 1.

Mean diameter	Surface functionality	Fluorescent?	Surface charge
0.49 μm	carboxylate-modified latex (CML)	yes	-262 μC/cm^2
0.95 μm	amidine	no	$+23.7$ μC/cm^2
1.2 μm	amidine	no	$+18.2$ μC/cm^2
1.5 μm	aldehyde-amidine	no	$+18.2$ μC/cm^2
2.1 μm	amidine	no	$+30.2$ μC/cm^2

Table 1: Charged particles used in electrostatic system experiments. Values for surface charge from data sheets provided by manufacturers.

A 100 μL sample of each colloid was diluted to 1% weight by volume. This was then vortexed for a few seconds and bath-sonicated for 10 seconds. We cleaned the particles by centrifuging and redispersing them several times in deionized (DI) water, using the following wash procedure.

1. Colloids were centrifuged for 5 minutes at 6600g.
2. Supernatant was removed and 190 μL of DI water were added to each sample.
3. Samples were vortexed for 5 seconds each and then bath-sonicated for 10 seconds.

Because the washing procedure involves centrifugation at high acceleration, it can cause the particles to aggregate. The vortexing and sonication steps break apart the majority of these aggregates, but some small aggregates remain and can later appear as clusters showing non-specific aggregation. We do not count these non-specific aggregates when we characterize the cluster size distribution.

We performed six wash cycles. After the last centrifugation, the supernatant was replaced with 40 μL of DI water, rather than 190 μL as before. Then 50 μL of 20 mM NaCl were added to each sample to achieve an overall salt concentration of 10 mM. This screens the repulsion between like particles before mixing.

We prepared mixtures of the positively and negatively charged particles such that each mixture contained one batch of positively charged particles at 1% w/v. In each mixture, the number

ratio of the large (positively charged) to small (negatively charged) spheres was 100 : 1. The salt concentration in each mixture was 10 mM NaCl. Each mixture consisted of large and small particles with a different size ratio α, as listed in Table 2.

α	Large particles	Small particles
1.94	0.95 μm amidine (+)	0.49 μm CML (-)
2.45	1.2 μm amidine (+)	0.49 μm CML (-)
3.06	1.5 μm aldehyde-amidine (+)	0.49 μm CML (-)
4.29	2.1 μm amidine (+)	0.49 μm CML (-)

Table 2: Size ratios and components of binary mixtures of charged colloids.

Each mixture was stored in a micro-centrifuge tube and vortexed at 3,000 RPM, bath-sonicated for 20 seconds, and then mounted on a Glas-Col Rugged Rotator to tumble slowly at 4°C. Each mixture tumbled for at least three days before observation to reduce the effects of sedimentation on local particle concentrations throughout the mixture. To make it easier to identify and characterize one cluster at a time, we diluted samples of the mixtures to 0.1% w/v just prior to observing the distribution of cluster sizes.

1.1 Electrostatics control experiment

In the experiments outlined above, each mixture contained particles with surface charges of opposite sign. In a separate control experiment, we mixed particles of two different sizes but with surface charges of the same sign. Both components in our control mixture were carboxylate-modified latex (CML) colloids with a size ratio $\alpha = 2.24$, as listed in Table 3.

Mean diameter	Surface functionality	Fluorescent?	Surface charge
0.49 μm	CML	yes	-262 μC/cm^2
1.1 μm	CML	no	-31.5 μC/cm^2

Table 3: Colloids used in electrostatic system control experiment.

These colloids were washed using the procedure outlined above and then mixed in a 100 : 1 number ratio. After tumbling at 4°C for several days, the cluster size distribution was measured. As shown in Figure 1, fewer than 1% of the small particles bind to large particles when they have surface charges of the same sign. Nonspecific aggregation is therefore rare in the charged colloidal systems.

1.2 Experiments without salt

In another set of experiments, mixtures of charged colloidal particles were prepared as described above, but without salt. The number ratio of positively charged spheres to negatively charged spheres was again 100 : 1, and several size ratios α were investigated, as listed in Table 4. As in the experiments with 10 mM NaCl, we tumbled the mixtures for several days before measuring the distribution of clusters.

Figure 2 shows that the average cluster sizes in these mixtures were smaller than the average sizes predicted from simulation and those observed in mixtures containing 10 mM NaCl. For instance,

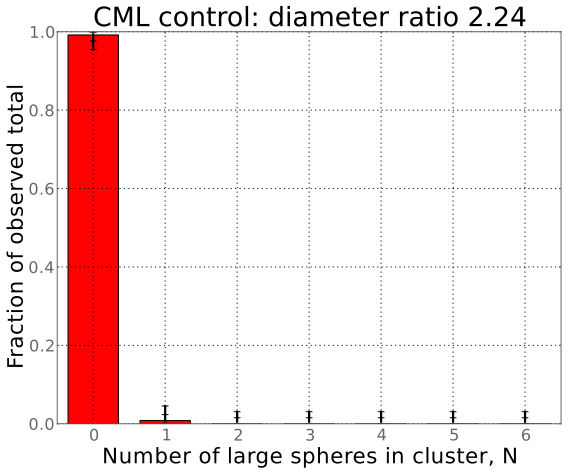

Figure 1: Cluster size distribution in a mixture of 1.1 μm non-fluorescent CML particles and 0.49 μm fluorescent CML particles in a 100 : 1 number ratio, showing that particles with surface charge of the same sign rarely form clusters.

α	Large particles	Small particles
1.09	1.2 μm amidine (+)	1.1 μm CML (-)
1.36	1.5 μm aldehyde-amidine (+)	1.1 μm CML (-)
1.94	0.95 μm amidine (+)	0.49 μm CML (-)
2.45	1.2 μm amidine (+)	0.49 μm CML (-)
3.06	1.5 μm aldehyde-amidine (+)	0.49 μm CML (-)
4.29	2.1 μm amidine (+)	0.49 μm CML (-)

Table 4: Size ratios and components of binary mixtures without salt.

at $\alpha = 2.45$ with 10 mM NaCl the average cluster size is $N = 3.9$, but when there is no salt in the system the average cluster size is $N = 2.7$. For the four size ratios for which there is data both without salt and with 10 mM NaCl, we found that clusters are 20% to 35% smaller when no salt is added.

These experiments show that electrostatic repulsion affects the cluster assembly. This observation is consistent with other recent experiments [4] showing that the cluster size distribution in binary mixtures depends on ionic strength when the salt concentration is less than 10 mM. In our mixtures with 10 mM NaCl, the Debye length is approximately 3 nm, very small compared to the particle sizes, so the large spheres do not interact with each other except at small distances. The random parking model should be more appropriate for systems like these where the interaction range is much smaller than the particle size. This is because the random parking model assumes no interactions between the particles except for a hard-core repulsion and irreversible binding on contact between spheres of two different types.

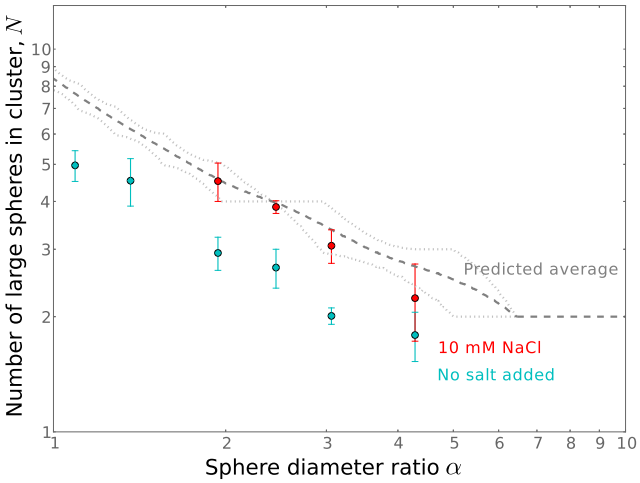

Figure 2: Average cluster sizes from simulations (dashed dark gray) and electrostatic experiments with (red data points) and without (cyan) salt. Widths of the cluster size distributions are indicated by dotted light gray lines for simulations and vertical error bars for experiments.

2 DNA-colloid experiments

In another set of experiments, we mixed small and large spheres labeled with complementary 65-base ssDNA oligonucleotides purchased from Integrated DNA Technologies:

- Sequence A: 5'-biotin-51xT-TGTTGTTAGGTTTA-3'
- Sequence B: 5'-biotin-51xT-TAAACCTAACAACA-3'

The oligonucleotides terminate with a biotin group, which allows us to graft them to streptavidin-coated polystyrene particles using a protocol from Dreyfus *et al.* [2]. The streptavidin-coated polystyrene particles are purchased from Bangs Laboratories, Inc. with the following diameters:

- 0.21 μm, fluorescent, to be coated with sequence B
- 0.39 μm, fluorescent, to be coated with sequence B
- 0.51 μm, fluorescent, to be coated with sequence B
- 0.97 μm, non-fluorescent, to be coated with sequence A

DNA strands were dissolved in water in 20 μM concentration. 20 μL of this DNA solution were mixed with 10 μL of 1% w/w streptavidin-coated polystyrene particles with 120 μL of phosphate buffer in a 1.7 mL propylene micro-centrifuge tube. Each 50 mL batch of buffer contained 0.0128 g KH_2PO_4, 0.0707 g K_2HPO_4, 0.1467 g NaCl, and 0.250 g F108 surfactant in 50 mL of deionized water. The buffer was filtered through a 0.2 μm membrane before use. A separate batch containing no salt was also prepared so that the salt concentration could be adjusted by combining the two.

Mixtures were vortexed at 3,000 RPM for 5 seconds and bath-sonicated for 10 seconds. They were incubated at room temperature for 30 minutes to allow the ssDNA to graft to the surface of the particles. Then we washed the colloids using the following procedure:

1. Colloids were centrifuged for 3 minutes at 12,000g.
2. Supernatant was removed and 100 μL of 50 mM NaCl buffer were added to each sample.
3. Samples were vortexed for 5 seconds each at 3,000 RPM and then bath-sonicated for 10 seconds.

As in the charged particle system, the centrifugation step can create aggregates, some of which survive the vortexing and sonication steps and appear as non-specifically aggregated clusters. We washed each colloid three times to remove excess DNA from the system, and then incubated each at 55°C for 30 minutes. We then washed three more times, incubated at 55°C for another 30 minutes, and washed three times again. At this point the salt concentration in the buffer was adjusted to 20 mM. The A- and B-labeled particles were mixed in a 100 : 1 (large : small) number ratio such that the larger particles were at a volume fraction of about 0.1%. Three separate mixtures were prepared, as listed in Table 5.

α	Large particles	Small particles
1.90	0.97 μm, sequence A	0.51 μm, sequence B
2.49	0.97 μm, sequence A	0.39 μm, sequence B
4.62	0.97 μm, sequence A	0.21 μm, sequence B

Table 5: Size ratios and components of mixtures with DNA-driven interactions.

After the mixtures had been prepared, we followed the same procedure that we used for the charged colloid system.

2.1 DNA-colloid control experiment

In the experiments outlined above, each mixture contained particles labeled with complementary DNA strands. In a separate control experiment, we mixed particles of two different sizes but labeled with identical ssDNA.

Both components in our control mixture were streptavidin-coated polystyrene colloids labeled with sequence A. We used 0.97 μm (non-fluorescent) and 0.51 μm (fluorescent) particles, yielding a size ratio $\alpha = 1.90$. The particles were functionalized with DNA using the same procedure described above and then mixed in a 100 : 1 number ratio. After tumbling at 4°C for several days, the cluster size distribution was measured. Figure 3 shows that fewer than 2% of the small spheres bind to large spheres when they are coated with the same DNA sequence. The low amount of nonspecific aggregation is expected, since we designed sequence A to have a negligible amount of self-hybridization even at 0°C.

3 Measurement of cluster size distribution

To measure the distribution of cluster sizes of a particular mixture, we placed a 5 μL, 0.1% w/v sample between two cover slips and then sealed it at the edges with UV-curable epoxy (Norland

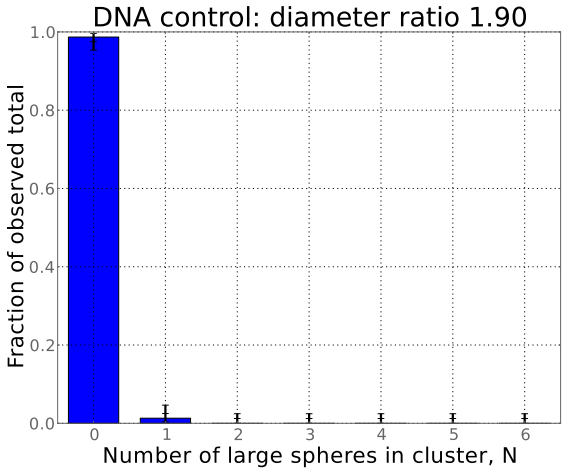

Figure 3: Cluster size distribution in a mixture of 0.97 μm non-fluorescent particles and 0.51 μm fluorescent particles in a 100 : 1 number ratio, coated with the same non-self-complementary DNA sequence (A).

Optical Adhesive 61). We observed each sample under differential interference contrast with a 100X oil-immersion objective on a Nikon Eclipse TE2000-E inverted microscope. We used fluorescence to identify the small spheres.

The distribution was obtained by counting the number of clusters at each N. $N = 0$ is a small sphere without any large spheres adsorbed, $N = 1$ a small sphere attached to a single large sphere, etc. We also counted clusters containing multiple small spheres and clusters formed through non-specific aggregation. The number of such clusters is small compared to the total number of clusters counted. Thus, we do not include these in the histograms.

Our counting procedure is designed to avoid errors from double counting. We begin by counting clusters in the field of view (FOV) on the microscope, scanning through z to find clusters that may initially be out of focus. The Brownian motion of each cluster eventually brings all particles into view. We can therefore determine the number of large and small spheres in each cluster through direct observation. Once we have recorded all clusters in the FOV, we translate the FOV to another part of the sample located more than one FOV away. We repeat this process to build up the histogram, rastering the FOV over the sample. We count more than 60 clusters at each size ratio and more than 120 clusters at size ratios greater than 2. The entire histogram for a given mixture is recorded in one session on the microscope.

4 Algorithm for simulating random sphere parking

We simulate the cluster distribution using an algorithm based on Monte Carlo trials. These consist of two stages:

Coarse stage We repeatedly try to insert a disc of radius $r = R_{\text{big}}/(R_{\text{big}} + R_{\text{small}})$ on the surface of the unit sphere. The center of the disc is randomly and uniformly distributed on the sphere. If the disc overlaps any discs that are already "parked", we reject it; otherwise we add it to the list of parked discs. After a fixed number of consecutive rejections, (typically $N_{\text{coarse}} = 10^4$), we switch to the fine stage.

Fine stage We compute the remaining regions of possible insertion, and then try to insert an additional disc. We choose the center of the disc randomly and uniformly from these regions.

To find the regions of possible insertion, we first compute the arcs that form their boundaries: Given a central disc of radius r, neighboring disc centers must lie on or outside a concentric circle of radius $2r$. We erase arcs that lie in the interior of the concentric circles of radius $2r$ about each neighboring disc. If the central circle contains any unerased arcs, these are added to our roster of arcs.

We do this for each parked disc center, and then stitch together the remaining arcs to form the regions to which another disc center could be added. To find the area of each region, we inscribe the region in a circumcircle and use a Monte-Carlo integration method to determine the ratio of the area of the region to the area of its circumcircle.

The algorithm terminates when the list of remaining arcs in the fine stage is empty, at which point the final number of inserted discs is recorded.

5 Calculating bounds on cluster size distribution

The upper and lower bounds $N_{\max}$ and $N_{\min}$ on the cluster size distribution can be calculated from *spherical codes* [3] corresponding to known solutions to the problems of spherical packings ($N_{\max}$) and spherical coverings ($N_{\min}$). Spherical packings are arrangements of N points on a unit sphere that maximize the smallest distance between any two of them [1, 3]. For a given α we determine $N_{\max}(\alpha)$ by looking up the spherical packing [3] with the largest N for which the minimal distance between points is at least $2\alpha/(1+\alpha)$. Our calculation of $N_{\min}(\alpha)$ is more involved, as explained below.

5.1 Connection between spherical covering and minimum parking

Here we verify that the best known coverings are also optimal solutions to the minimum parking problem. For a given configuration of n "parked" points on a unit sphere, let the *covering radius* be the maximum distance between any point on the sphere to the nearest parked point. Let the *packing radius* be (half) the minimum of the pairwise distances between the parked points. If the parked points represent centers of circles with some radius r, it is impossible to add another circle without overlapping a parked one if and only if the covering radius is less than $2r$. The circles that are already parked do not overlap provided that the packing radius is greater than r. Therefore, if we are given an optimal solution to the covering problem, that is, one that minimizes the covering radius for a given n, it will also be the optimal minimal parking configuration if the covering radius is less than 2 times the packing radius.

We manually verify that the best known coverings satisfy this constraint for $n = 4, \ldots, 130$ by calculating the packing radius for each optimal known covering, obtained from ref. [3]. Table 6 shows the covering radius, packing radius, and difference (in degrees). The difference is always positive, confirming our statement.

n	2 * packing radius	covering radius	2*(packing radius) - (covering radius)
4	109.47	70.53	38.94
5	90.00	63.43	26.57
6	90.00	54.74	35.26
7	72.00	51.03	20.97
8	61.76	48.14	13.62
9	68.97	45.88	23.09
10	65.53	42.31	23.22
11	50.65	41.43	9.22
12	63.43	37.38	26.06
13	46.23	37.07	9.16
14	52.58	34.94	17.64
15	45.67	34.04	11.63
16	50.48	32.90	17.58
17	41.63	32.09	9.54
18	45.53	31.01	14.51
19	40.73	30.37	10.36
20	40.01	29.62	10.39
21	39.45	28.82	10.62
22	40.70	27.81	12.89
23	38.99	27.48	11.51
24	36.67	26.81	9.86
25	36.75	26.33	10.42
26	35.12	25.84	9.27
27	38.06	25.25	12.81
28	35.87	24.66	11.21
29	33.86	24.37	9.50
30	31.18	23.88	7.30
31	29.94	23.61	6.33
32	37.38	22.69	14.69
33	26.61	22.59	4.02
34	30.82	22.33	8.49
35	27.98	22.07	5.90
36	28.78	21.70	7.08
37	31.22	21.31	9.91
38	30.31	21.07	9.24
39	30.73	20.85	9.87
40	30.13	20.47	9.66
41	27.71	20.32	7.39
42	28.34	20.05	8.29
43	27.27	19.84	7.43
44	26.36	19.64	6.72
45	25.15	19.42	5.73
46	29.11	19.16	9.96

47	25.38	18.99	6.38
48	27.70	18.69	9.01
49	24.93	18.59	6.33
50	28.01	18.30	9.71
51	24.30	18.20	6.10
52	24.24	18.05	6.19
53	22.56	17.88	4.68
54	25.58	17.68	7.90
55	24.06	17.52	6.54
56	24.89	17.35	7.54
57	23.98	17.18	6.80
58	23.72	17.02	6.70
59	23.69	16.90	6.79
60	24.67	16.77	7.90
61	20.50	16.64	3.86
62	20.43	16.49	3.94
63	21.60	16.37	5.23
64	21.34	16.19	5.15
65	20.78	16.11	4.66
66	21.61	15.96	5.66
67	21.32	15.86	5.46
68	21.74	15.72	6.02
69	20.41	15.60	4.82
70	21.47	15.50	5.98
71	21.46	15.39	6.07
72	23.06	15.14	7.92
73	17.51	15.12	2.39
74	17.95	15.03	2.92
75	20.02	14.95	5.07
76	19.08	14.85	4.23
77	22.03	14.74	7.29
78	19.14	14.66	4.49
79	19.77	14.56	5.21
80	19.94	14.45	5.49
81	19.07	14.38	4.69
82	20.40	14.29	6.11
83	17.08	14.22	2.86
84	19.93	14.12	5.81
85	19.92	14.05	5.88
86	19.89	13.96	5.93
87	18.70	13.88	4.81
88	19.80	13.79	6.01
89	19.76	13.71	6.05
90	19.83	13.62	6.21
91	17.18	13.56	3.62
92	17.83	13.49	4.34

93	18.75	13.43	5.32
94	19.15	13.35	5.81
95	18.54	13.29	5.25
96	19.21	13.21	6.00
97	18.38	13.14	5.24
98	18.99	13.06	5.93
99	19.06	13.00	6.06
100	18.58	12.94	5.64
101	18.67	12.87	5.80
102	17.63	12.81	4.82
103	17.51	12.74	4.77
104	18.49	12.67	5.82
105	18.94	12.62	6.32
106	17.66	12.56	5.10
107	18.62	12.50	6.13
108	18.10	12.43	5.67
109	18.23	12.38	5.85
110	18.40	12.30	6.10
111	18.70	12.25	6.45
112	18.71	12.19	6.52
113	18.28	12.15	6.14
114	16.87	12.10	4.78
115	17.42	12.05	5.37
116	16.27	11.99	4.28
117	17.67	11.94	5.73
118	17.71	11.89	5.83
119	17.09	11.84	5.25
120	17.25	11.79	5.47
121	17.56	11.73	5.83
122	17.70	11.68	6.02
123	14.38	11.64	2.74
124	14.14	11.59	2.55
125	17.38	11.54	5.84
126	17.07	11.49	5.58
127	16.54	11.45	5.09
128	16.50	11.41	5.09
129	16.98	11.36	5.62
130	16.95	11.32	5.63

Table 6: Packing and covering radii for different cluster sizes n, measured in degrees, and the differences between them. Because the differences are always positive, we conclude that the optimal covering configuration is also the optimal minimal parking configuration, at least for $N \in \{4, \ldots, 130\}$.

References

[1] J. H. Conway and N. J. A. Sloane. *Sphere Packings, Lattices and Groups*. Springer-Verlag, New York, 1993.

[2] R. Dreyfus, M. E. Leunissen, R. Sha, A. V. Tkachenko, N. C. Seeman, D. J. Pine, and P. M. Chaikin. Simple quantitative model for the reversible association of DNA coated colloids. *Phys. Rev. Lett.*, 102(4):048301, Jan 2009.

[3] N. J. A. Sloane, R. H. Hardin, and W. D. Smith. Tables of spherical codes. Published electronically at www.research.att.com/∼njas/packings/, 2011.

[4] Y. Wang, G. Chen, M. Yang, G. Silber, S. Xing, L. H. Tan, F. Wang, Y. Feng, X. Liu, S. Li, and H. Chen. A systems approach towards the stoichiometry-controlled hetero-assembly of nanoparticles. *Nat. Commun.*, 1(87), 2010.